Catalytic Co-pyrolysis of cellulosic ethanol processing residue with high-density polyethylene over biomass bottom ash catalyst

Bo Chen [a,b], Zhitong Yao [c], Changwei Zhang [b], Shikun Cheng [d], Mengying Zhu [b], Yankun Wang [b], Yilu Wu [b], Hui Cao [b], Ian Watson [a], Di Cai [b,*]

[a] Systems, Power and Energy Research Division, James Watts School of Engineering, College of Science and Engineering, James Watt South, University of Glasgow, Glasgow, G128QQ, UK

[b] National Energy R&D Center for Biorefinery, Beijing University of Chemical Technology, Beijing, 100029, PR China

[c] College of Materials Science and Environmental Engineering, Hangzhou Dianzi University, Hangzhou 310018, China

[d] Beijing Key Laboratory of Resource-Oriented Treatment of Industrial Pollutants, University of Science and Technology Beijing, Beijing 100083, PR China

* Corresponding authors

Emails: caidibuct@163.com (Di Cai)

Abstract:

In this study, the bagasse ash (BA) from biorefinery process was recovered ad used as a catalyst in the co-pyrolysis of solid residue from second-generation bioethanol plant with high-density polyethylene (HDPE). The co-pyrolytic behaviors were studied using thermogravimetric analyzer at three heating rates of 10, 20, and 40 K min^{-1}. The synergistic effects between BA and HDPE and their co-pyrolysis kinetics were investigated using two model-free methods, Kissinger-Akahira-Sunose (KAS) and Flynn-Wall-Ozawa (FWO). The pyrolysis products were determined by pyrolysis-gas chromatography/mass spectrometry (Py-GC/MS) as well. The results indicated that the addition of BA could increase the production yield. The average apparent active energy (Ea) of co-pyrolysis was 171.3 kJ mol^{-1} from KAS and 174 kJ mol^{-1} from FWO, which were lower than that for catalyst-free pyrolysis (174.8 kJ mol^{-1} from KAS and 177.3 kJ mol^{-1} from FWO). The novel co-pyrolysis process showed great potential in improving both the economic and environment sides of the second-generation biorefineries.

Key words:

Ethanol process residual;

Bottom ash;

Plastic;

Co-pyrolysis;

Biorefinery

Statements and Declarations

The authors have no competing interests to declare that are relevant to the content of this article.

1. Introduction

The depletion of fossil-based energy and the growing emissions of greenhouse gases caused urgent need to develop alternative renewable biofuels [1–4]. Lignocelluloses, the abundant biomass materials, are considered as an ideal feedstock for biochemical production [5]. Compared to direct use of lignocellulosic biomass for biofuels production, utilizing the solid residual from second-generation bioethanol plant can significantly improve the economic feasibility of biorefineries and simplify the downstream solid waste management [6–8]. In a typical second-generation bioethanol plant using corn cob as the feedstock, the ethanol-processing residue (EPR) is remained as a solid waste after saccharification and fermentation. Due to the high content of lignin and non-hydrolysable holocellulose in EPR, it also can be considered as an ideal feedstock for biofuels production [9].

Among different lignocelluloses conversion routes, pyrolysis is regarded as one of the most promising methods due to a series of advantages such as processing simplicity and great feedstock flexibility [10–12]. However, the crude bio-oil obtained from the biomass pyrolysis process can not directly replace the traditional fuel due to the high oxygenates content, acidity, and corrosiveness [13, 14]. To improve crude bio-oil quality, one of the commonly adopted methods is the bio-oil deoxygenation by hydrodeoxygenation and catalytic deoxygenation [15]. Nonetheless, these processes are always possessed high hydrogen consumption, which increase the economic costs

[16]. Another method that always suggested to upgrade the crude bio-oil is introducing hydrogen-rich materials such as waste plastic and co-pyrolysis with lignocellulosic biomass materials [17]. In this process, plastic could provide hydrogen during the co-pyrolysis process and prohibits the coke formation because of the appropriate H/C_{eff} ratio [12, 18, 19]. In addition, co-pyrolysis of biomass and waste plastics is also environmentally friendly as it reduces carbon emissions and offers innovative ideas for end-of-life strategies and energy extraction for waste plastics [17].

In order to further improve the quality of bio-oil, catalytic co-pyrolysis of biomass and waste plastic is advocated [20, 21]. Various commercial catalysts, e.g., zeolites [22], dolomite [23] Ni-based catalysts [24] have been used to upgrade bio-oil by co-pyrolysis. However, the economic feasibility of catalytic co-pyrolysis was long been criticized by the high cost and low recyclable catalysts. Currently, many researchers focus on using solid waste. For instance, Loy et al. used industrial waste coal bottom ash as a catalyst in catalytic pyrolysis of rice husk, the results illustrated that the using coal bottom ash as catalyst could increase the syngas production and decrease coke formation, and the hydrogen was increased by 8.4 % [25]. In another work, Wu et al. used incineration bottom ash as catalyst in catalytic pyrolysis of biogas residue. The results suggested incineration bottom ash had negative effect on biogas residue pyrolysis [26]. Similar to the aforementioned researches, the bottom ash (BA), which is from the combustion of EPR to generate heat or electricity to

power the biorefinery process, also exhibited great potential to be reused as a catalyst to upgrade bio-oil and decrease the activation energy of pyrolysis reactions [21, 27]. This is because it contains high silica content and mesoporous surface area, which could improve the pyrolysis performance [28]. In addition, other impurities such as lime, alkalis, iron oxide, alumina are also contained in BA to ensure the good pyrolysis performance [21].

In fact, benefits from the EPR pyrolysis are obvious. For instance, part of the EPR obtained in the biorefinery process can be used as a pyrolysis feedstock, while another part can be burned to supply heat to the upstream processes, and the combustion product BA can be reused as a catalyst in the pyrolysis process. On this basis, combining the pyrolytic bio-oil production with conventional biorefinery process, solid residues produced in the typical second-generation biorefinery process, including the EPR and BA, can be utilized as feedstock and catalyst, respectively, so as to realize 'zero emission' of solid waste.

To better investigated the pyrolysis behaviours of EPR, TGA is the simplest and quickest method to gain the complete profile of non-isothermal thermal decomposition process [29]. The kinetic parameters such as activation energy, pre-exponential factor and order of reaction can be determined from TGA experiments whether using model-free or model-fitting models. Model-free methods can provide estimation of kinetic parameters without knowledge of the reaction mechanism [30]. Model-fitting methods are to find the model which give the best fit to the

thermogravimetric data the from different pyrolysis model to further calculate kinetic parameters [31]. Compared to model-fitting methods, model-free methods produce more accurate estimation of activation energy in lignocellulosic biomass pyrolysis because model-fitting methods are based on single heating rate [32]. Among the model-free methods, Kissinger–Akahira–Sunose (KAS), Flynn–Wall–Ozawa (FWO), Friedman and Starink methods are the most commonly adopted methods [32, 33].

In the present work, aiming to extend the entire second-generation bio-ethanol process, the EPR and high-density polyethylene (HDPE) are utilized as feedstocks for pyrolytic bio-oil production. During the process, BA was recycled and further reused as catalyst for the co-pyrolysis of EPR/HDPE blends (**Fig.1**). To better understand the chemical and physical properties of EPR and BA, the chemical composition was characterised by Brunauer–Emmett–Teller analysis (BET), Fourier transform infrared spectroscopy (FT-IR), X-ray fluorescence (XRF), Field emission scanning electron microscope (FESEM), and Energy disperse X-ray analysis (EDX).

Thermogravimetric analyser (TGA) was conducted to investigate the pyrolysis characteristics of catalytic co-pyrolysis and non-catalytic co-pyrolysis of EPR/HDPE. Two model-free methods (KAS and FWO) are used to calculate the activation energy of pyrolysis process. The product distribution from the pyrolysis process was characterized by Py-GC/MS.

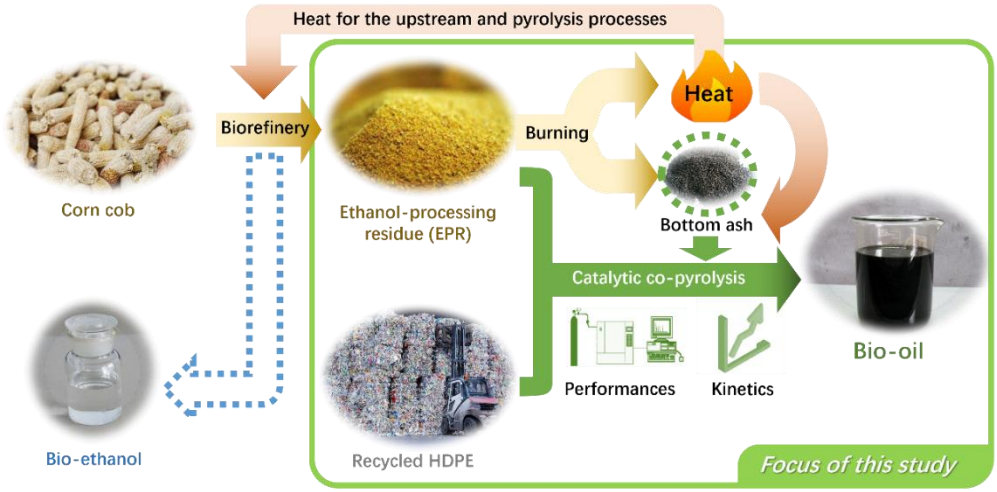

Fig.1 Diagram for the co-pyrolysis of EPR and HDPE by BA.

2. Materials and methods

2.1 Materials

The EPR from the corn cob biorefinery process and BA were obtained from Longlive Biotech Co., Ltd., China. The BA was collected after the burning of EPR for heat. The high-density polyethylene (HDPE 600) was purchased from Beijing Jinma Plastic Co. Ltd., China. Density and melting point of HDPE were 0.956 g cm^{-3} and 136 ℃, respectively. The EPR and BA were first dried at 105 ℃ for 24 h, followed by milling into particles with average size of less than 20 μm.

2.2 Experimental

The ultimate analysis of the moisture, volatiles, fixed carbon and ash content in

EPR were determined by an element analyzer (CHN628, LECO, USA). The components of EPR were analyzed by the method of the National Renewable Energy Laboratory of USA [26]. The functional groups of EPR were evaluated by Fourier-transform infrared spectrometer (FT-IR) (Nicolet 6700, Thermo Fisher, USA) in the range of 500 cm^{-1} to 4000 cm^{-1} with a resolution of 4 cm^{-1}. N_2 adsorption measurements were conducted by a gas sorption system (Autosorb-iQ, Quantachrome, USA). Micropore volume and pore diameter were calculated by the t-plot method and DFT method, respectively.

The field emission scanning electron microscope (FESEM, Hitachi SU8020) integrated with energy disperse spectrometer (EDS, IXRF 550i) were used to observe the surface morphology and measure the elemental composition of EPR and BA. N_2 adsorption were conducted to measure the pore volume and diameter by a gas sorption system (Autosorb-iQ, Quantachrome, USA). Samples were degassed at 150 °C for 6 h and measured at 77 K. Total pore volume were obtained from the resulted isotherms. Micropore volume and pore diameter were calculated by the t-plot method and DFT method, respectively.

TGA (LECO TGA701) was carried out to evaluate the thermal decomposition behavior of EPR/HDPE blend and EPR/HDPE/BA blend. The EPR/HDPE blend was mixed in the ratio of 1:1 meanwhile the EPR/HDPE/BA blend was mixed in the ratio of 1:1:0.1. The samples were heated from room temperature to 700 °C at three different heating rates (10, 20, 40 K min^{-1}) in N_2 atmosphere. Each experiment was

carried out in triplicate.

As for the analysis of the pyrolysis product, gas chromatography/mass spectrometry (Py-GC/MS) was adopted. The initial temperature of pyrolysis reactor (CDS 5000) was 300 ℃. Temperature was increased to 600 ℃ at a heating rate of 1 ℃ ms^{-1} and held at 600 ℃ for additional 20 s. The chromatography separation of the pyrolysis vapors was conducted using a VF-17MS capillary column (30 m×250 μm×0.25 μm, length, OD, ID respectively). The injector temperature was 300 °C and the split ratio was 80:1. The initial column temperature was set at 40 °C and maintained for 12 s. After that, the column temperature was increased to 200 °C at a rate of 5 °C min^{-1}, followed by increase to 300 °C at a rate of 20 °C min^{-1}. Helium was used as the carrier gas at a flow rate of 1 mL min^{-1}. The mass spectra were operated at an electron energy of 70 eV from molecular mass of 35 u to 500 u. The compounds in the Py-GC/MS spectrum were identified according to the National Institute of Standards and Technology (NIST) mass spectrometry database.

2.3 Kinetics

2.3.1 Kinetic theory

The pyrolysis process of solid-state feedstocks such as biomass and plastic waste can be treated as a single reaction: Biomass and/or plastic → volatiles + char.

The kinetic equation for the transformation rate from solid state to volatiles can be expressed as:

$$\frac{d\alpha}{dt} = k(t)f(\alpha) \quad (1)$$

where k is the reaction rate constant, $f(\alpha)$ is the reaction model, t is reaction time and α is conversion rate, which can be calculated by:

$$\alpha = \frac{m_0 - m_t}{m_0 - m_f} \quad (2)$$

where m_0, m_t and m_f are the initial mass, mass at time *t* and final sample mass, respectively. Substituting the Arrhenius formula into Eq. (1), the following equation is obtained:

$$\frac{d\alpha}{dt} = Aexp\left(\frac{-E}{RT}\right)f(\alpha) \quad (3)$$

where A is the pre-exponential factor, *R* is the gas constant, *E* is the activation energy (kJ mol^{-1}). *T* is the absolute temperature (K).

As for the non-isothermal TGA analysis, the heating rate β can be defined as:

$$\beta = \frac{dT}{dt} \quad (4)$$

Combining Eq.3 with Eq.4, Eq.5 is obtained:

$$\frac{d\alpha}{dT} = \frac{A}{\beta}exp\left(\frac{-E}{RT}\right)f(\alpha) \quad (5)$$

2.3.2 Model-free methods

The KAS method is an integration method derived from Murray and White approximation [34, 35], and is expressed as:

$$ln\left(\frac{\beta}{T^2}\right) = ln\frac{AR}{Eg(\alpha)} - \frac{E}{RT} \quad (6)$$

where $g(\alpha)$ is the integrated form of $f(\alpha)$. It is a constant at given conversion rate. The activation energy *E* can be estimated by the slopes of the $\frac{1}{T}$ versus $ln\left(\frac{\beta}{T^2}\right)$ plots.

The FWO method is based on Doyle's approximation [36], and it can be expressed by the following equation:

$$ln(\beta) = ln\frac{0.0048AE}{Rg(\alpha)} - \frac{1.0516E}{RT} \quad (7)$$

where *E* can be obtained from the slope of the $\frac{1}{T}$ versus $ln(\beta)$ plots as well.

3. Results and discussion

3.1 EPR and BA characterization

The chemical compositions of EPR are listed in **Table 1**. It contains 58.8 wt% of cellulose, 5.4 wt% of hemicellulose, and 22.5 wt% of lignin. The high cellulose content and low hemicellulose could be attributed to the hydrolysis of hemicellulose during the acid pretreatment and delignification during the alkali pretreatment before simultaneous saccharification fermentation [6]. Because of the resistant corn cob structure, the raw material, the inaccessible holocellulose by cellulase remains in the EPR. Compared with the negligible ash content in the raw corn cob (3.2 wt%), the ash content in EPR was relatively high, owing to the residual yeast cells and salts [6].

According to the proximate analysis, EPR has a high volatile matter content (59.76 wt%), which would be leading to an elevated amount of pyrolysis products and

decrease the yield of solid products [20, 37]. Moreover, even though the EPR theoretically contains proteins and cells debris, the N and S contents were extremely low (1.8 wt% and 0.5 wt%, respectively), indicating there would be low emission of NO_x and SO_2 in the pyrolysis progress.

Table 1 Physical and chemical properties of EPR.

Index	Values	Unit
Chemical composition [a]		
Cellulose	58.8±2.3	%
Hemicellulose	5.4±0.1	%
Lignin	22.5±0.9	%
Soluble substances	5.1±0.2	%
Ash	8.2±0.1	%
Proximate analysis [a]		
Moisture	7.05	%
Volatile matter	59.76	%
Fixed carbon	15.61	%
Ash	17.58	%
Ultimate analysis [b]		
C	48.70	%
H	4.97	%

O*	19.39	%
N	1.80	%
S	0.506	%
BET analysis [c]		
Surface area	3.015	m^2/g
Cumulative pore volume	0.027	cc/g
Average pore diameter	3.312	nm

[a] On dry mass fraction basis (wt%).

[b] On dry and ash-free basis (wt%).

[c] BJH absorption.

[*] Calculated by difference.

The FT-IR spectrum of EPR was also analyzed. The large band between 3000 cm^{-1} and 3750 cm^{-1} belongs to the O-H stretching vibration of hydroxyl of cellulose and hemicellulose [38]. The peak located at 2920.88 cm^{-1} is attributed to C-H stretching vibration of methyl or methylene group [39]. In addition, the peak around 1648.24 cm^{-1} is the C=O stretching which indicated the aromatic groups of lignin, and the peak at 1512.03 cm^{-1} is evidence of benzene skeletal vibration of lignin [6]. The peak arising from 1061.89 cm^{-1} belongs to the C-O stretching vibration of cellulose and hemicellulose [39]. Therefore, EPR had a large amount of aromatic and oxygenated functional groups (**Fig. S1**).

The surface morphology and elemental composition of EPR were analyzed. It exhibited a rough surface after acid pretreatment and enzymatic hydrolysis process, and there are many different sizes of cracks and pore cavities afforded to the adhesion of BA with feedstock. The EDS analysis illustrated that the EPR is mainly containing C (56.67 wt%) and O (32.29 wt%) elements (**Fig.S2**). Furthermore, a small amount of alkali metals such as Na (3.60 wt%) was also determined, which could be assigned to the residual salts after fermentation (**Table S1**).

The XRF analysis of BA indicated that it is mainly composed of SiO_2 (52.95 wt%) (**Table S2**). Moreover, high content of alkali metal oxides such as CaO (10.32 wt%), K_2O (10.11 wt%), MgO (3.11 wt%) and Na_2O (2.24 wt%) are also detected. Transition metal oxides (e.g., Fe_2O_3) and amphoteric metal oxides (e.g., Al_2O_3) were also detected. Since alkali metal oxides always prohibited coke formation on catalyst [40], whilst the Fe_2O_3 and Al_2O_3 could enhance the syngas production [21], therefore, the BA can be potentially used as catalyst for improve the pyrolysis behavior of EPR [41].

The SEM analysis indicated that the BA exhibits a porous structure, and there are many small particles disperse on the surface. The porous and agglomerated structure of BA increases the contact area with biomass [42]. The elemental compositions of BA are shown in **Table 2**, which showed the C and O contents are 32.23 wt% and 25.62 wt%, respectively, whereas the content of Si is 13.76 wt% (**Fig. S3**). The BET surface area, pore volume and diameter of BA are further determined (**Table S3**). The

average pore diameter of BA is 3.710 nm, indicating that BA is mainly consisted of mesoporous material [43]. The cumulative pore volume of BA is 0.101 cc g^{-1}, which is much higher than that of the traditional catalysis such as Ni (0.019) and CaO (0.0016) [43]. Furthermore, the surface area of BA is 11.038 m^2 g^{-1}, it is also higher than fresh nickel (4.68 m^2 g^{-1}) and natural zeolite (1.25 m^2 g^{-1}) [25]. According to Loy's work [25], the higher BET surface area of BA would provide more active sites for the co-pyrolysis of EPR and HDPE, which driven us to further investigate the co-catalytic performances of the EPR/HDPE/BA blend.

Table 2 EDS analysis of BA.

Element	Content（wt%）
C	32.23
O	25.62
Si	13.76
Fe	5.33
Ca	5.18
Al	4.48
K	4.23
Cl	3.31
Na	3.08
Mg	2.78

3.2 Co-pyrolysis of EPR and HDPE

Fig. 2 shows the TGA and DTG patterns of the EPR/HDPE/BA blends. The BA-free process is treated as the control (refers to the non-catalytic pyrolysis process). As it can be observed in **Fig. 2a**, both the non-catalytic and catalytic pyrolysis processes present similar degradation trends. Generally, the thermal degradation of EPR/HDPE in both two groups that are with and without BA can be divided into four stages. In the temperature range of room temperature (~25 ℃) to 150 ℃, the weight loss is mainly attributed to thermally driving off the moisture and light volatile compounds in EPR. In addition, hemicellulose begins to decompose at this stage because of its loose structure [6]. The second stage occurs in the temperature range of 200-380 ℃. In this stage, cellulose and hemicellulose decomposed rapidly. Hemicellulose has a relatively loose structure, because it consists of saccharides such as glucose and xylose, and exhibited an amorphous structure that can be easily degraded [44]. Whereas, cellulose consists of long-chain polymers, glucose, which exhibit a more stable structure than other components. Hence, the decomposition temperature of cellulose is higher than hemicellulose [45]. The strong and sharp peak located at 472 ℃ belongs to the degradation of HDPE [46]. The slow degradation of lignin almost exists in the whole pyrolysis process, since lignin has a stable structure with aromatic rings [21]. It has been reported that the decomposition of lignin releases

much CH_4 and H_2 due to the presence of aromatic ring and O–CH_3 functional group [47].

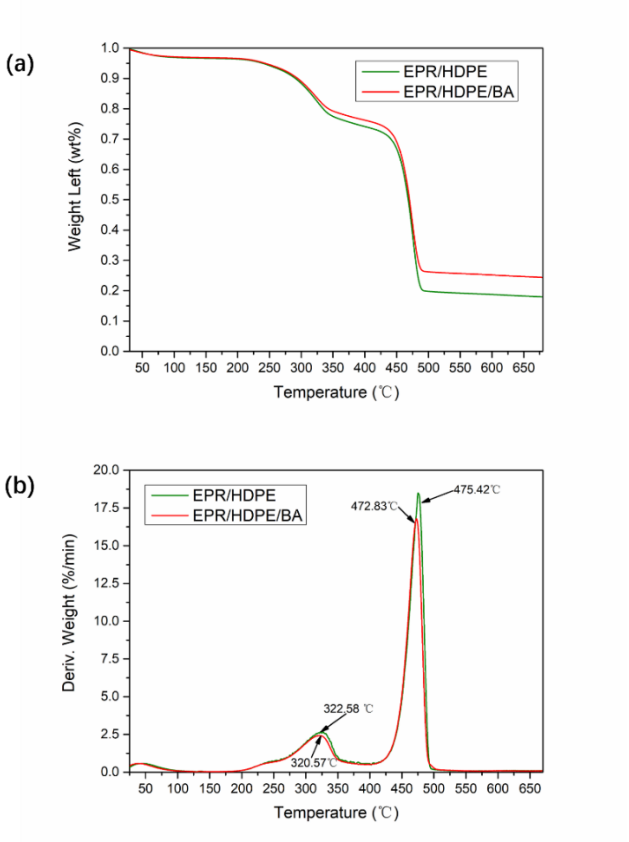

Fig. 2 TGA-DTG profiles of EPR and HDPE co-pyrolysis with and without BA.

The DTG curves of EPR/HDPE and EPR/HDPE/BA are presented in **Fig. 2b**. It can be observed that the DTG curve of EPR/HDPE is similar with the curve obtained in EPR/HDPE/BA. Compared with the non-catalytic pyrolysis, the peak temperature shifts to slightly lower temperature after adding BA. Moreover, the maximum degradation rate decreases when BA was added into the pyrolysis of EPR/HDPE. It has been reported that the maximum degradation rate is one of the most important

factors for the reduction of the energy consumption in the pyrolysis process [25]. Thus, it is affirmed that BA has a synergistic effect in the pyrolysis of EPR/HDPE blends.

3.3 Py-GC-MS analysis

Py-GC-MS analysis was carried out to investigate the pyrolysis products from EPR/HDPE blends and the effect of BA. The main compositions of the pyrolysis product can be classified into aromatics, ketone, furan, hydrocarbon, alcohols and other substances. The relative abundances of these compositions are shown in **Fig.3**, and the detailed products are listed in **Table S4**. There is no acetic acid in both catalytic and non-catalytic pyrolysis products, and the abundance of ketones are low. This phenomenon can be attributed to the low content of hemicellulose in EPR. It is demonstrated that acid is produced from the cracking of the acetyl group in hemicellulose, and ketones are also generated after hemicellulose degradation [48, 49]. Alcohols are mainly produced from the decomposition of hemicellulose and cellulose [50]. Attributed to the abundant cellulose content in the EPR, the concentration of alcohols is relatively higher than other products. The highest content found in both the catalytic and non-catalytic pyrolysis samples is hydrocarbon, which is attributed to the decomposition of HDPE.

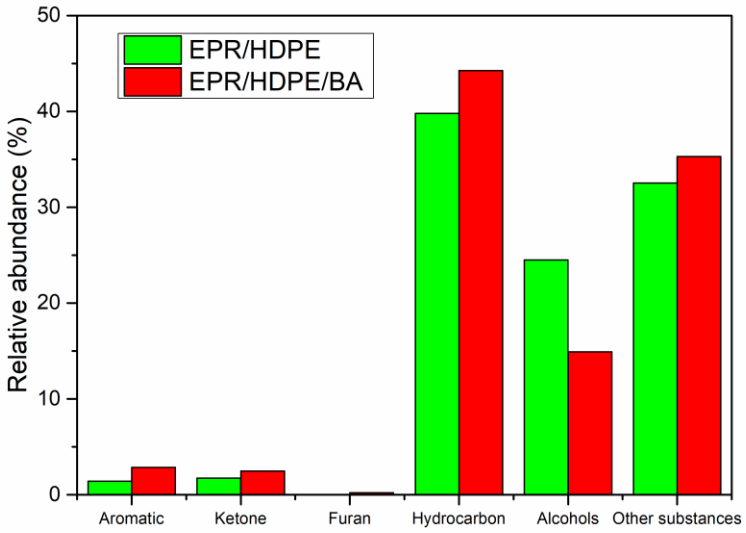

Fig. 3 Pyrolysis products of EPR and HDPE co-pyrolysis with and without BA.

The aromatic hydrocarbons from catalytic pyrolysis are higher than that from non-catalytic pyrolysis, owing to the acidity and size selectivity of BA [51]. It also can be observed that the presence of BA enhanced the production of hydrocarbons. Hydrocarbons are often regarded as valuable products from biomass pyrolysis. The enhancement of hydrocarbons production indicates that the BA facilitated the pyrolysis of biomass. Catalytic pyrolysis of biomass is usually carried out by breaking of C-CO(OH) and C-OH bonds in dehydration, decarbonylation and decarboxylation reactions [52]. After adding BA, the production of alcohols is decreased significantly (**Fig.3**). BA may deoxygenate the pyrolysis products in terms of lowering the yield of alcohols. All these points indicate that BA can be used as a catalyst in co-pyrolysis of EPR and HDPE.

3.4 Kinetic analysis

Compared to model-fitting methods, model-free methods are more accurate for non-linear reaction mechanism study [53]. Hence, KAS and FWO methods were chosen to calculate the activation energy. Because of the unstable decomposition reaction at the start and end of pyrolysis process, the conversion rate (α) from 0.1 to 0.9 is selected [44]. The kinetic parameters including apparent activation energy (Ea) and the coefficients of determination (R^2) are shown in **Table 3**. The Ea values are distinct between different conversion rates due to the various energy requirements of the reactions occurring during the pyrolysis process [54]. Based on the KAS method, the linear model of non-catalytic and catalytic co-pyrolysis of EPR and HDPE is determined by plotting $\frac{1}{T}$ versus $ln\left(\frac{\beta}{T^2}\right)$ (**Fig. 4a** and **4b**). All the points fitted well with R^2 ranging from 0.971 to 1.0 (**Table 3**). Therefore, the first order reaction mechanism was suitable for both non-catalytic and catalytic EPR/HDPE pyrolysis. The average E value for non-catalytic pyrolysis of EPR/HDPE is 174.8 kJ mol^{-1}, which is higher than that of catalytic pyrolysis of EPR/HDPE using BA (insert value, kJ mol^{-1}). Activation energy is the minimum energy requirement for a reaction to start [21]. A reaction with a low E value can increase the reaction rate and energy efficiency [55]. Thus, the results indicate that BA has a positive effect on the activation energy reduction.

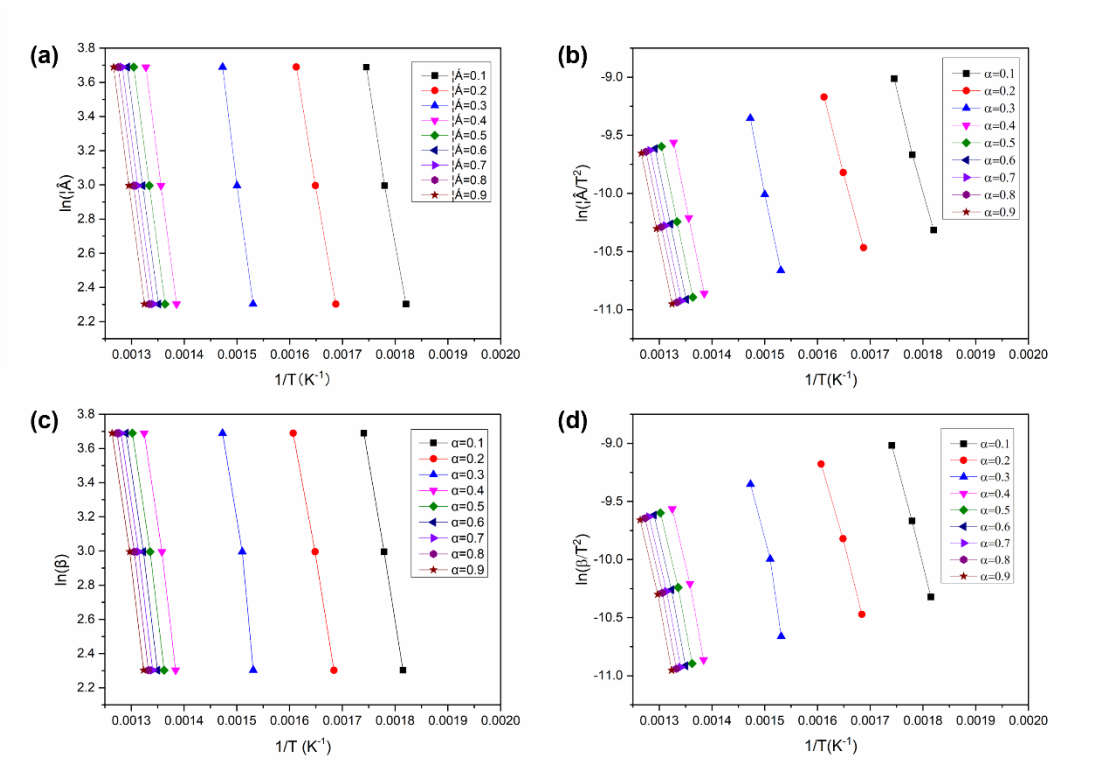

Fig.4 Linear correlation of co-pyrolysis of EPR and HDPE by FWO and KAS methods. (a) EPR/HDPE (KAS); (b) EPR/HDPE/BA (KAS); (c) EPR/HDPE (FWO); (d) EPR/HDPE/BA (FWO).

To ensure the reliability of the kinetic parameters, another model-free method, the FWO kinetic method is adopted. The linear relationships for the given conversion rate are determined by the plots of $\frac{1}{T}$ versus $ln(\beta)$ (**Fig. 4c** and **4d**). As shown in **Table 3**, the *Ea* values estimated by FWO method are slightly higher than that of KAS method. The R^2 values in FWO method are all greater than 0.97, which is similar with the results obtained by KAS method. The results reaffirm the first-order reaction mechanism fitted well with both non-catalytic pyrolysis of EPR/HDPE and catalytic pyrolysis of EPR/HDPE using BA. By the catalysis of BA, the *Ea* value

decreased from 177.3 kJ mol^{-1} to 174.0 kJ mol^{-1}. The results are in good agreement with KAS method. In both KAS and FWO method, the average *E* value decreased with the presence of BA as catalyst. This phenomenon can be attributed to the suitable porous structure and the chemical composition of BA (**Fig. 3** and **Table 3**). Additionally, the metal oxides and char component in BA would further boost the decomposition reaction [21]. Overall, the *E* values estimated by KAS and FWO methods are similar, which demonstrate the reliability of the experimental data. Therefore, the addition of BA in EPR/HDPE blends could reduce the *E* value of the co-pyrolysis process.

Table 3 *Ea* and R^2 values corresponding to α for EPR/HDPE co-pyrolysis

	Catalytic co-pyrolysis of EPR/HDPE				Non-catalytic co-pyrolysis of EPR/HDPE			
α	KAS		FWO		KAS		FWO	
	E (J mol^{-1})	R^2	*E* (J mol^{-1})	R^2	*E* (J mol^{-1})	R^2	*E* (J mol^{-1})	R^2
0.1	143.7	0.999	145.5	0.999	146.2	0.997	147.9	0.998
0.2	143.6	0.997	146.1	0.998	138.9	1.000	141.7	0.999
0.3	188.0	0.971	189.3	0.974	181.3	0.999	182.9	0.999
0.4	185.8	0.994	188.3	0.994	180.4	1.000	182.9	1.000
0.5	181.6	0.995	184.4	0.995	178.5	1.000	181.6	1.000
0.6	181.7	0.995	184.7	0.996	178.9	0.999	182.0	0.999
0.7	181.0	0.995	184.1	0.996	178.4	1.000	181.7	1.000

0.8	182.8	0.996	185.9	0.996	180.2	1.000	183.5	1.000
0.9	184.7	0.995	187.8	0.996	178.8	1.000	182.1	1.000
Average	174.8	-	177.3	-	171.3	-	174.0	-

4. Conclusion

The thermal characteristics, pyrolysis products distribution and kinetic parameters of co-pyrolysis of EPR and HDPE using recycled BA as catalyst were studied. According to the TGA results, the addition of BA reduced the peak temperature and the maximum degradation rate of pyrolysis. These results indicated that adding BA could reduce the *Ea* value of EPR and HDPE co-pyrolysis (171.3 kJ mol^{-1} (KAS) and 174 kJ mol^{-1} (FWO) for catalytic co-pyrolysis, 174.8 kJ mol^{-1} (KAS) and 177.3 kJ mol^{-1} (FWO) for catalyst-free co-pyrolysis), and thereby improving the reaction rate and energy efficiency. The catalytic co-pyrolysis of EPR and HDPE using BA provide a route to converting EPR to bioenergy in a low-cost manner with inexpensive, sustainable catalyst material, which showed the potential in connection with the biorefinery process for 'zero' solid waste and improvement of the eco-feasibility. In future work, the EPR/HDPE ratio and the usage of BA in catalytic co-pyrolysis process will be optimized. In addition, master-plot method would be adopted to obtain the reaction model and calculate pre-exponential factor.

Declarations

Ethical Approval

Not applicable

Competing Interests

The authors have no competing interests to declare that are relevant to the content of this article.

Author information

Authors and Affiliations

Systems, Power and Energy Research Division, James Watts School of Engineering, College of Science and Engineering, James Watt South, University of Glasgow, Glasgow, G128QQ, UK

Bo Chen, Ian Watson

National Energy R&D Center for Biorefinery, Beijing University of Chemical Technology, Beijing, 100029, PR China

Bo Chen, Changwei Zhang, Mengying Zhu, Yankun Wang, Yilu Wu, Hui Cao

College of Materials Science and Environmental Engineering, Hangzhou Dianzi University, Hangzhou 310018, China

Shikun Cheng

Beijing Key Laboratory of Resource-Oriented Treatment of Industrial Pollutants, University of Science and Technology Beijing, Beijing 100083, PR China

Zhitong Yao

Contributions

Conceptualization: Bo Chen, Di Cai; methodology: Bo Chen, Mengying Zhu, Yilu Wu; formal analysis and investigation: Bo Chen, Changwei Zhang, Yankun Wang, Shikun Cheng; writing—original draft preparation: Bo Chen; writing—review and editing: Bo Chen, Zhitong Yao, Di Cai, Ian Watson; funding acquisition: Bo Chen, Hui Cao, Di Cai; supervision: Di Cai, Ian Watson.

Corresponding author

Correspondence to Di Cai

E-mail: caidibuct@163.com

Fundings

This work was funded by the National Key Research and Development Program of China (Grant No. 2018YFB1501702), the National Natural Science Foundation of China (Grant No. 22078018), and the Bingtuan Science and Technology Program (Grant No. 2022DB025), and China Scholarship Council (Grant No. 201906880041).

Availability of data and materials

Data supporting the findings of this study are available from the corresponding author Di Cai on request.

References

1. Menares T, Herrera J, Romero R, et al (2020) Waste tires pyrolysis kinetics and reaction mechanisms explained by TGA and Py-GC/MS under kinetically-controlled regime. Waste Management 102:21–29. https://doi.org/https://doi.org/10.1016/j.wasman.2019.10.027
2. Mishra RK, Mohanty K, Wang X (2020) Pyrolysis kinetic behavior and Py-GC–MS analysis of waste dahlia flowers into renewable fuel and value-added chemicals. Fuel 260:116338. https://doi.org/https://doi.org/10.1016/j.fuel.2019.116338
3. Zheng YW, Tao L, Yang XQ, et al (2018) Study of the thermal behavior, kinetics, and product characterization of biomass and low-density polyethylene co-pyrolysis by thermogravimetric analysis and pyrolysis-GC/MS. J Anal Appl Pyrolysis 133:185–197
4. Parada MP, Osseweijer P, Duque JAP (2017) Sustainable biorefineries, an analysis of practices for incorporating sustainability in biorefinery design. Ind Crops Prod 106:105–123
5. Shao J, Jia C, Chen X, et al (2019) Enhancing the Production of Light Olefins from Wheat Straw with Modified HZSM-5 Catalytic Pyrolysis. Energy & Fuels. https://doi.org/10.1021/acs.energyfuels.9b02945
6. Chen B, Cai D, Luo ZF, et al (2018) Corncob residual reinforced polyethylene composites considering the biorefinery process and the enhancement of performance. J Clean Prod 198:452–462
7. Virmond E, de Sena RF, Albrecht W, et al (2012) Characterisation of agroindustrial solid residues as biofuels and potential application in thermochemical processes. Waste Management 32:1952–1961. https://doi.org/https://doi.org/10.1016/j.wasman.2012.05.014
8. Cristóbal J, Caldeira C, Corrado S, Sala S (2018) Techno-economic and profitability analysis of food waste biorefineries at European level. Bioresour Technol 259:244–252. https://doi.org/https://doi.org/10.1016/j.biortech.2018.03.016
9. Yao Z, Cai D, Chen X, et al (2022) Thermal behavior and kinetic study on the co-pyrolysis of biomass with polymer waste. Biomass Convers Biorefin. https://doi.org/10.1007/s13399-022-02480-7
10. Zhang CW, Wen H, Chen CJ, et al (2019) Simultaneous saccharification and juice co-fermentation for high-titer ethanol production using sweet sorghum stalk. Renew Energy 134:44–53
11. Chen CJ, Cai D, Qin PY, et al (2018) Bio-plasticizer production by hybrid acetone-butanol-ethanol fermentation with full cell catalysis of Candida sp. 99-125. Bioresour Technol 257:217–222

12. Kim YM, Jae J, Kim BS, et al (2017) Catalytic co-pyrolysis of torrefied yellow poplar and high-density polyethylene using microporous HZSM-5 and mesoporous Al-MCM-41 catalysts. Energy Convers Manag 149:966–973
13. Guizani C, Valin S, Billaud J, et al (2017) Biomass fast pyrolysis in a drop tube reactor for bio oil production: Experiments and modeling. Fuel 207:71–84. https://doi.org/https://doi.org/10.1016/j.fuel.2017.06.068
14. Weng J, Cheng Z, Zhang Y, et al (2023) Online evaluation of catalytic co-pyrolysis of hemicellulose and polypropylene over CaO catalyst. Fuel 332:125993. https://doi.org/https://doi.org/10.1016/j.fuel.2022.125993
15. Du H, Yu Q, Liu G, et al (2022) Catalytic deoxygenation of carboxyl compounds in the hydrothermal liquefaction crude bio-oil via in-situ hydrogen supply by CuO-CeO2/γ-Al2O3 catalyst. Fuel 317:123367. https://doi.org/https://doi.org/10.1016/j.fuel.2022.123367
16. Chen W, Luo Z, Yu C, et al (2014) Upgrading of bio-oil in supercritical ethanol: Catalysts screening, solvent recovery and catalyst stability study. J Supercrit Fluids 95:387–393. https://doi.org/https://doi.org/10.1016/j.supflu.2014.09.041
17. Ahmed MHM, Batalha N, Mahmudul HMD, et al (2020) A review on advanced catalytic co-pyrolysis of biomass and hydrogen-rich feedstock: Insights into synergistic effect, catalyst development and reaction mechanism. Bioresour Technol 310:123457. https://doi.org/https://doi.org/10.1016/j.biortech.2020.123457
18. Wu XY, Wu YL, Wu KJ, et al (2015) Study on pyrolytic kinetics and behavior: The co-pyrolysis of microalgae and polypropylene. Bioresour Technol 192:522–528
19. Zhang XS, Lei HW, Zhu L, et al (2016) Thermal behavior and kinetic study for catalytic co-pyrolysis of biomass with plastics. Bioresour Technol 220:233–238
20. Balasundram V, Ibrahim N, Kasmani RM, et al (2017) Thermogravimetric catalytic pyrolysis and kinetic studies of coconut copra and rice husk for possible maximum production of pyrolysis oil. J Clean Prod 167:218–228
21. Loy ACM, Gan DKW, Yusup S, et al (2018) Thermogravimetric kinetic modelling of in-situ catalytic pyrolytic conversion of rice husk to bioenergy using rice hull ash catalyst. Bioresour Technol 261:213–222
22. Mishra RK, Mohanty K (2020) Pyrolysis of Manilkara zapota seeds over ZSM-5 to produce high-quality bio-oil and chemicals. Fuel 280:. https://doi.org/10.1016/j.fuel.2020.118594
23. Wang P, Shen Y (2022) Catalytic pyrolysis of cellulose and chitin with calcined dolomite – Pyrolysis kinetics and products analysis. Fuel 312:. https://doi.org/10.1016/j.fuel.2021.122875
24. Deng Z, Syed-Hassan SSA, Chen Y, et al (2022) Effect of Ni/Al2O3 mixing on the coking behavior of bio-oil during its pyrolysis: Further understanding based on the interaction between its components. Fuel 315:.

https://doi.org/10.1016/j.fuel.2022.123136
25. Loy ACM, Yusup S, Lam MK, et al (2018) The effect of industrial waste coal bottom ash as catalyst in catalytic pyrolysis of rice husk for syngas production. Energy Convers Manag 165:541–554
26. Wu W, Zhang R, Wang Z, et al (2022) Catalytic pyrolysis of biogas residues with incineration bottom ash by TG-MS: Kinetics analysis and biochar stability. Fuel 322:124253. https://doi.org/https://doi.org/10.1016/j.fuel.2022.124253
27. Sutrisno B, Hidayat A (2016) Upgrading of bio-oil from the pyrolysis of biomass over the rice husk ash catalysts. IOP Conf Ser Mater Sci Eng 162:12014. https://doi.org/10.1088/1757-899x/162/1/012014
28. Prasara-A J, Gheewala SH (2017) Sustainable utilization of rice husk ash from power plants: A review. J Clean Prod 167:1020–1028. https://doi.org/https://doi.org/10.1016/j.jclepro.2016.11.042
29. Liew JX, Loy ACM, Chin BLF, et al (2021) Synergistic effects of catalytic co-pyrolysis of corn cob and HDPE waste mixtures using weight average global process model. Renew Energy 170:. https://doi.org/10.1016/j.renene.2021.02.053
30. Majid M, Chin BLF, Jawad ZA, et al (2021) Particle swarm optimization and global sensitivity analysis for catalytic co-pyrolysis of Chlorella vulgaris and plastic waste mixtures. Bioresour Technol 329:. https://doi.org/10.1016/j.biortech.2021.124874
31. Ding Y, Zhang Y, Zhang J, et al (2019) Kinetic parameters estimation of pinus sylvestris pyrolysis by Kissinger-Kai method coupled with Particle Swarm Optimization and global sensitivity analysis. Bioresour Technol 293:. https://doi.org/10.1016/j.biortech.2019.122079
32. Iqbal A, Badshah SL, Alves JLF, et al (2022) An insight into the thermokinetics of the pyrolysis of invasive grass Sorghum halepense towards its bioenergy potential. Biomass Convers Biorefin. https://doi.org/10.1007/s13399-022-02697-6
33. Badshah SL, Shah Z, Francisco Alves JL, et al (2021) Pyrolysis of the freshwater macroalgae Spirogyra crassa: Evaluating its bioenergy potential using kinetic triplet and thermodynamic parameters. Renew Energy 179:. https://doi.org/10.1016/j.renene.2021.07.105
34. Kissinger HE (1957) Reaction Kinetics in Differential Thermal Analysis. Anal Chem 29:1702–1706. https://doi.org/10.1021/ac60131a045
35. Starink MJ (2003) The determination of activation energy from linear heating rate experiments: a comparison of the accuracy of isoconversion methods. Thermochim Acta 404:163–176
36. Doyle CD (1962) Estimating isothermal life from thermogravimetric data. J Appl Polym Sci 6:639–642. https://doi.org/10.1002/app.1962.070062406
37. Ghetti P, Ricca L, Angelini L (1996) Thermal analysis of biomass and

corresponding pyrolysis products. Fuel 75:565–573
38. Nadlene R, Sapuan SM, Jawaid M, et al (2018) The effects of chemical treatment on the structural and thermal, physical, and mechanical and morphological properties of roselle fiber-reinforced vinyl ester composites. Polym Compos 39:274–287. https://doi.org/https://doi.org/10.1002/pc.23927
39. Liu R, Peng Y, Cao J, Chen Y (2014) Comparison on properties of lignocellulosic flour/polymer composites by using wood, cellulose, and lignin flours as fillers. Compos Sci Technol 103:1–7. https://doi.org/https://doi.org/10.1016/j.compscitech.2014.08.005
40. Sahraei OAZ, Larachi F, Abatzoglou N, Iliuta MC (2017) Hydrogen production by glycerol steam reforming catalyzed by Ni-promoted Fe/Mg-bearing metallurgical wastes. Applied Catalysis B-Environmental 219:183–193
41. Gan LH, Goldfarb JL (2019) Solid waste to biofuels and heterogeneous sorbents via pyrolysis of wheat straw in the presence of fly ash as an in situ catalyst. J Anal Appl Pyrolysis 137:96–105
42. Herman AP, Yusup S, Shahbaz M, Patrick DO (2016) Bottom Ash Characterization and its Catalytic Potential in Biomass Gasification. In: Procedia Engineering
43. Khan Z, Yusup S, Ahmad MM (2014) Performance Study of Ni Catalyst with Quicklime (CaO) as CO2 Adsorbent in Palm Kernel Shell Steam Gasification for Hydrogen Production. Proceedings of the International Conference on Process Engineering and Advanced Materials 2012-Icpeam 2012 917:283–291. https://doi.org/10.4028/www.scientific.net/AMR.917.283
44. Cai H, Liu J, Xie W, et al (2019) Pyrolytic kinetics, reaction mechanisms and products of waste tea via TG-FTIR and Py-GC/MS. Energy Convers Manag 184:436–447. https://doi.org/https://doi.org/10.1016/j.enconman.2019.01.031
45. Gu X, Ma X, Li L, et al (2013) Pyrolysis of poplar wood sawdust by TG-FTIR and Py–GC/MS. J Anal Appl Pyrolysis 102:16–23. https://doi.org/https://doi.org/10.1016/j.jaap.2013.04.009
46. Burra KG, Gupta AK (2018) Kinetics of synergistic effects in co-pyrolysis of biomass with plastic wastes. Appl Energy 220:408–418
47. Yang HP, Yan R, Chen HP, et al (2007) Characteristics of hemicellulose, cellulose and lignin pyrolysis. Fuel 86:1781–1788
48. Huber GW, Iborra S, Corma A (2006) Synthesis of Transportation Fuels from Biomass: Chemistry, Catalysts, and Engineering. Chem Rev 106:4044–4098. https://doi.org/10.1021/cr068360d
49. Chen W-H, Wang C-W, Kumar G, et al (2018) Effect of torrefaction pretreatment on the pyrolysis of rubber wood sawdust analyzed by Py-GC/MS. Bioresour Technol 259:469–473. https://doi.org/https://doi.org/10.1016/j.biortech.2018.03.033
50. Chen H, Xie Y, Chen W, et al (2019) Investigation on co-pyrolysis of lignocellulosic biomass and amino acids using TG-FTIR and Py-GC/MS.

Energy Convers Manag 196:320–329. https://doi.org/https://doi.org/10.1016/j.enconman.2019.06.010
51. Pattiya A, Titiloye JO, Bridgwater A v (2008) Fast pyrolysis of cassava rhizome in the presence of catalysts. J Anal Appl Pyrolysis 81:72–79. https://doi.org/https://doi.org/10.1016/j.jaap.2007.09.002
52. Lin Y-C, Huber GW (2009) The critical role of heterogeneous catalysis in lignocellulosic biomass conversion. Energy Environ Sci 2:68–80. https://doi.org/10.1039/B814955K
53. Yap TL, Loy ACM, Chin BLF, et al (2022) Synergistic effects of catalytic co-pyrolysis Chlorella vulgaris and polyethylene mixtures using artificial neuron network: Thermodynamic and empirical kinetic analyses. J Environ Chem Eng 10:. https://doi.org/10.1016/j.jece.2022.107391
54. Aslan DI, Ozogul B, Ceylan S, Geyikci F (2018) Thermokinetic analysis and product characterization of Medium Density Fiberboard pyrolysis. Bioresour Technol 258:105–110
55. Ozsin G, Putun AE (2017) Insights into pyrolysis and co-pyrolysis of biomass and polystyrene: Thermochemical behaviors, kinetics and evolved gas analysis. Energy Convers Manag 149:675–685